Study of the Conformational Change of Amylose Induced by Complexation with Iodine Using Synchrotron X-ray Small-Angle Scattering

Toshihiro Hirai,*,† Mitsuhiro Hirai,‡ Sadao Hayashi,† and Tatsuo Ueki§

Faculty of Textile Science and Technology, Shinshu University, 3-15-1 Tokida, Ueda-shi 386, Japan, Faculty of General Studies, Gunnma University, 4-2 Aramaki-cho, Maebashi-shi 371, Japan, and The Institute of Physical and Chemical Research, 2-1 Hirosawa, Wako-shi 351-01, Japan

Received December 30, 1991
Revised Manuscript Received July 22, 1992

Introduction

Amylose has been known to form a blue complex with iodine in the presence of iodide in aqueous solution.[1] The crystal structure of the amylose–iodine complex reveals a clathrate, in which the polyiodine is included in the helical cavity of the amylose.[2,3] The structure of the iodine complex of cyclodextrin was also investigated in detail as a model of the iodine complex of amylose.[4–7]

However, the structure of the complex in aqueous solution is still ambiguous in spite of many investigations.[1,5,7–32] The fundamental structure of the complex in aqueous solution is believed to be basically the same as in the crystal or solid form with the polyiodine in the channel of the helix. The structure change on complexation has also been investigated from various points of view.[1,2a–f,5,11,19,25–28,30,32] In this paper, we tried to study it by using small-angle X-ray scattering of the synchrotron orbital radiation (SOR). This technique allows us to follow the structure change in the solution accompanying complexation. The results were obtained after eliminating the strong background due to the scattering by heavy atoms, illustrating the effectiveness of the strong X-ray beam of SOR.

Experimental Section

Materials and Complexation of Amylose with Iodine. Amyloses were purchased from Nakarai Chemicals Co., with molecular weights of 2900 and 16 000, which were designated by AMA and AMB, respectively. Other chemicals used were reagent grade and were used without further purification. Iodine complexes of the amyloses were prepared by mixing the amylose aqueous solution of iodine and iodide. In order to obtain sufficient scattering intensity and a shorter irradiation time, the polymer concentration was kept as high as possible, and the polymers were solubilized in a 1 N KOH aqueous solution. The irradiation time should be short to avoid gelation of the polymer solution. The concentrations of the stock polymer solutions were 10.0 wt % for AMA and 3.00 wt % for AMB, respectively. In the case of AMB, because of the high viscosity of the stock solution, we had to reduce the concentration to the low value given above. Right before the complexation the polymer stock solution was neutralized to pH 7.0 with acetic acid and diluted if needed. The concentrations of the neutralized polymer solutions were 9.5 and 0.74 wt % for AMA and AMB, respectively.

The complex solutions, with $[I_2]/[KI] = 0.10$, were prepared by addition of an aliquot of a stock solution containing 0.2 M KI and 0.02 M I_2. Iodine binding affinities of AMA and AMB were estimated as 1 mg of I_2/100 mg of polymer and 20 mg of I_2/100 mg of polymer, respectively, according to Banks et al.[33,34] The iodine concentration added was varied from below saturation to above saturation. The ionic strength of the complex solutions prepared were 0.53 ± 0.04 and 0.14 ± 0.01 for AMA and AMB, respectively. Polymer concentrations of the complex solutions were 4.7 and 0.37 wt % for AMA and AMB, respectively. Measurements were carried out 10 min after the complexation.

Small-Angle X-ray Scattering Measurements. Small-angle X-ray scattering measurements used a synchrotron radiation X-ray scattering spectrometer for enzymes at the National Laboratory for High Energy Physics, Ttsukuba, Japan. The X-ray beam is monochromatized by using a double-crystal monochromator and focused with a toroidal focusing mirror. Scattering data are recorded by using a one-dimensional position-sensitive proportional counter with a probe 20 cm in effective length. We used 1.49-Å radiation and a sample-to-detector distance of 65 cm. Slit corrections were not carried out because quasi-point-type optics were used. The details of the optics and instruments are given elsewhere.[35] Samples were contained in a quartz cell with 1-mm path length, and the temperature of the sample holder was maintained at 15.0 ± 0.1 °C by circulating water. Exposure time was 900 s for each sample. The electron current in the storage ring was 140–250 mA.

Scattering Data Analysis

The calibrated scattering intensity $I(q)$ from particles is obtained from

$$I(q) = \frac{I_{sol}(q)}{C_{sol}T_{sol}} - \frac{I_{solv}(q)}{C_{solv}T_{solv}} \quad (1)$$

where $q = 4\pi(\sin\theta)/\lambda$, 2θ, λ, $I_{sol}(q)$, $I_{solv}(q)$, C_{solv}, C_{solv}, T_{sol}, and T_{solv} represent the scattering angle, wavelength, the scattering intensities of the solution and pure solvent, the incident X-ray beam intensities for the solution and for the solvent monitored using the ion chamber just in front of the sample cell, and the X-ray beam transmissions through the samples, respectively. The suffixes, sol and solv, refer to the solution and the solvent, respectively. The T values are estimated by use of the X-ray mass absorption coefficients of the elements in the samples.

The $I(q)$ values were corrected first by analysis of the beginning of the scattering curve by using the Guinier equation

$$I(q) = I(0)\exp(-q^2R_g^2/3) \quad (2)$$

where $I(0)$ designates the zero-angle scattering intensity and R_g is the radius of gyration.[36]

The zero-angle scattering intensity, $I(0)$, is proportional to the square of the total particle scattering amplitude and can be expressed in the form

$$I(0) \propto |\int_V \{\rho(r) - \rho_s\}\,dr|^2 = |\int_V \rho'(r)\,dr|^2 = (\bar{\rho}V)^2 \quad (3)$$

where $\rho(r)$, ρ_s, $\rho(r)$, and ρ are the scattering density distribution of the particle, the average scattering density of the solvent, and the excess scattering density distribution of the particle with respect to ρ_s and its average scattering density (so-called "contrast"), respectively.[37]

The radius of gyration, R_g, is defined as

$$R_g^2 = \int_V \rho(r)r^2\,dr / \int_V \rho(r)\,dr \quad (4)$$

To determine R_g values and $I(0)$ intensities, we used the least-squares method for the Guinier plot, $\ln I(q)$ vs q^2 in the q range 0.020–0.035 Å^{-1}.

The second analysis for the total scattering curve is carried out by calculating the distance distribution func-

* To whom correspondence should be addressed.
† Shinshu University.
‡ Gunnma University.
§ The Institute of Physical and Chemical Research.

0024-9297/92/2225-6699$03.00/0

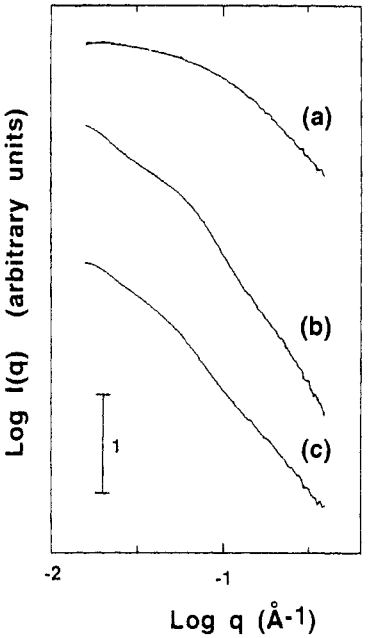

Figure 1. Observed small-angle X-ray scattering curves of amylose–iodine complexes at a series of iodine concentrations. Molecular weight = 2900 (abbreviated as AMA). $10^3[I_2]$ (mol/L) = (a) 0, (b) 2.0, (c) 6.0. [amylose] = 0.29 (unit mol)/L, $[I_2]/[KI]$ = 1/10 at 15 °C.

tion, $p(r)$. The function $p(r)$ is given by Fourier inversion of the scattering intensity $I(q)$ as

$$p(r) = \frac{2}{\pi}\int_0^\infty rqI(q)\sin(rq)\,dq \qquad (5)$$

It depends both on the particle geometry, expressing the set of distances joining the volume elements within a particle, and on a particle inner inhomogeneity distribution. In calculating the functionm $p(r)$, the extrapolation method using the Guinier plot was applied for the small-angle data sets and the modified intensity as

$$I'(q) = I(q)\exp(-kq^2) \qquad (6)$$

(k, an artificial damping factor, was used so as to remove the Fourier truncation effect.) The maximum diameter, D_{max}, of the particle can be estimated from the $p(r)$ function satisfying the condition $p(r) = 0$ for $r > D_{max}$.

Results and Discussion

The log $I(q)$ vs log q plots in Figures 1 and 2 show the scattering curves of the iodine complexes, AMA and AMB, as a function of iodine concentrations. In Figures 1–4, (a)–(c) correspond to the scattering curve of native solution with 0 mol/L $[I_2]$, an iodine complex solution with a medium concentration of I_2, and an iodine complex solution with the highest concentration of I_2, respectively. By comparison of the profiles of these plots, it can be seen that in the case of AMA the scattering curve is changed drastically, suggesting a structural change of the AMA molecule. In the case of AMB there is no major change in the scattering curve, so the structural change of the AMB molecule was assumed to be small.

According to the Guinier plots, as shown in Figures 3 and 4, the R_g value of AMA increased remarkably from 20.5 to 41.1 Å, whereas that of AMB decreased slightly from 58.5 to 55.1 Å. Using eq 3 the ratio of the volume change on complexation with iodine can be estimated by comparison of zero-angle scattering intensities. At a constant molar concentration c of AMA the zero-angle

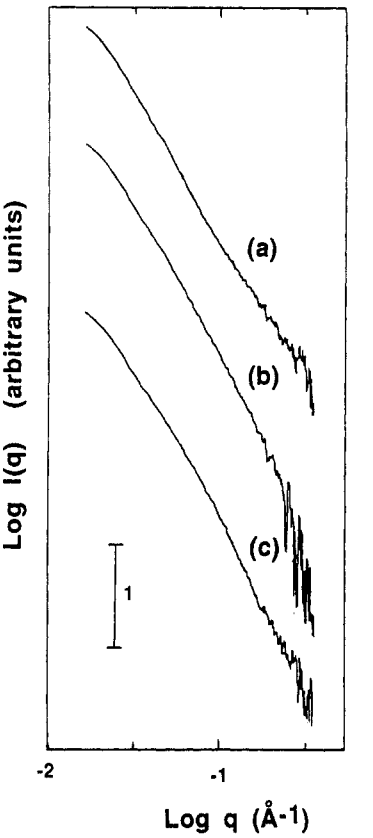

Figure 2. Observed small-angle X-ray scattering curves of amylose–iodine complexes at a series of iodine concentrations. Molecular weight = 16 000 (abbreviated as AMB). $10^4[I_2]$ (mol/L) = (a) 0, (b) 6.0, (c) 20.0. [amylose] = 0.023 (unit mol)/L, $[I_2]/[KI]$ = 1/10 at 15 °C.

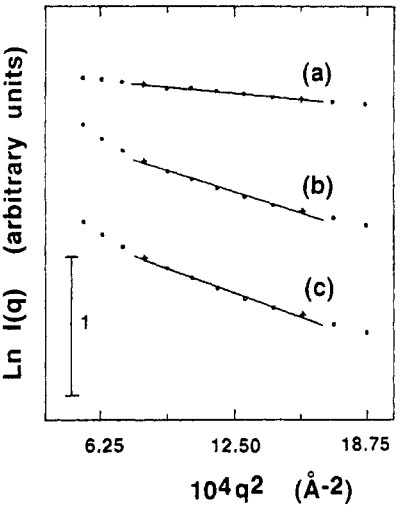

Figure 3. Guinier plots for the scattering curves in Figure 1. The marks used correspond to those in Figure 1. The straight lines obtained by the least-squares method for Guinier plots in the q range 0.03–0.04 $Å^{-1}$ are used to determine R_g and $I(0)$ intensities.

scattering intensity of oligomer made up of n AMA molecules, $I_{ol}(0)$, is given by

$$I_{ol}(0) = \frac{c}{n}(n\bar{\rho}V)^2 = nc(\bar{\rho}V)^2 = nI(0) \qquad (7)$$

where we can neglect the change of the contrast accompanying the amylose–iodine complexation. The difference of the average scattering density between the complex and its solvent and that for the native solution have approximately the same value because the increase in the average scattering density for solvent, {ρ[1 N KOH + 0.006

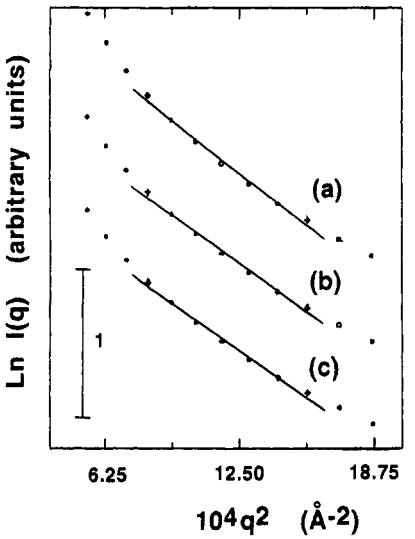

Figure 4. Guinier plots for the scattering curves in Figure 2. The marks used correspond to those in Figure 2. The straight lines obtained by the least-squares method for Guinier plots in the q range 0.03–0.04 Å^{-1} are used to determine R_g and $I(0)$ intensities.

M I_2 + 0.06 M KI] − ρ[1 N KOH]}/ρ[1 N KOH], is 8.5 × 10^{-3} and that for solute, {ρ[AMA] − ρ[I–AMA]}/ρ[AMA], is 7.2 × 10^{-3} according to iodine binding affinities of AMA 1 mg of I_2/100 mg of polymer. The contribution to the variation in zero-angle scattering intensity by the change of the contrast is then below 1%, smaller than the experimental errors. Therefore the ratio of the volume change is proportional to the ratio, $nI_{ol}(0)/I(0)$, and $n \approx 9$ was obtained by our experiments.

The distance distribution functions calculated by using eq 5 are shown in Figure 5a,b for AMA and AMB. As seen from Figure 5a, in the case of AMA, the maximum diameter D_{max} which corresponds to the length of the intraparticle vector, increased from 85 to 158 Å, accompanying the shift of the center of the $p(r)$ function to longer distances. The insert, Figure 5c, shows the calculated $p(r)$ functions of the model structures for AMA at $[I_2] = 0$ and 0.6 × 10^{-2} M. The model for AMA at $[I_2] = 0$ M is a cylinder with radius 14.6 Å and height 61.4 Å, and that for for AMA at $[I_2] = 0.6 \times 10^{-2}$ M is an ellipsoid of rotation with semiaxes 33.2 and 79.0 Å. The parameters of those models are adopted so that the R_g values and the shapes of the $p(r)$ functions coincide with those obtained from the scattering data. The ratio of volume of these two models is 8.9/1, which in the range of experimental error agrees well with experiments, $n \approx 9$. This suggests that for AMA the complexation with iodine induces an aggregation of several complexes to an anisotropic structure. In the case of AMB, as shown in Figure 5b, the circumstances are quite different. The slight decrease of the maximum diameter D_{max} from 181 to 173 Å was not accompanied by a change of the shape of the $p(r)$ functions, suggesting aggregation. The results described above are summarized in Table I.

It may be concluded that the AMB structure changes by the addition of iodine from an extended helix to a more tightly wound form, as inferred previously.[17,18,29,34]

However, AMA, which aggregates somewhat even in the absence of iodine, aggregates further on addition of iodine to an ellipsoidal structure by stacking the AMA molecules, as in cyclodextrin–iodine complexes.[5,6]

Acknowledgment. We are grateful to Professor T. Matsushita and Dr. Y. Amemiya of the Photon Factory at the National Laboratory for High Energy Physics for the initial setting of the optics and CAMAC data aquisition system. This work was performed under the approval of the Photon Factory Programme Advisory Committee (Proposal No. 87-149).

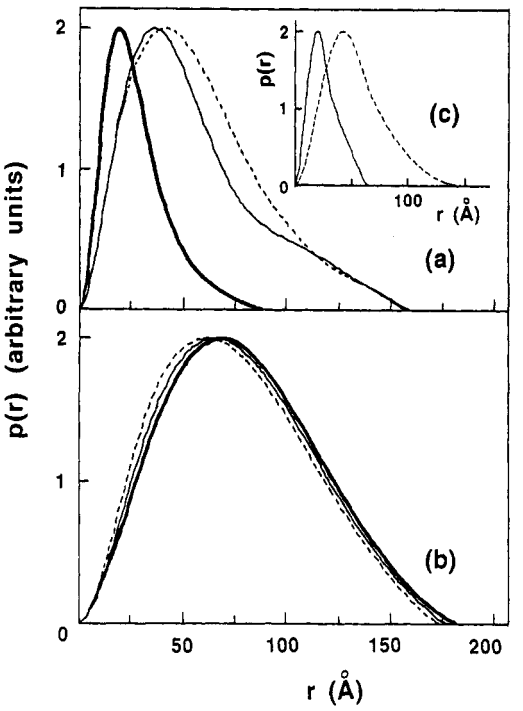

Figure 5. Distance distribution functions, $p(r)$, of AMA–iodine complexes (a) and AMB–iodine complexes (b) as a function of $[I_2]$ concentration (mol/L): full line, thin line, and broken line refer to $[I_2] = 0$, $[I_2] = 0.2 \times 10^{-2}$, and $[I_2] = 0.6 \times 10^{-2}$, respectively, in the case of AMA and to $[I_2] = 0$, $[I_2] = 0.6 \times 10^{-3}$, and $[I_2] = 0.2 \times 10^{-2}$, respectively, in the case of AMB. These $p(r)$ functions are calculated with the scattering curves obtained by using the extrapolation method and the artificial damping factor. The insert (c) shows the $p(r)$ function of the model structures for AMA–iodine complexes corresponding to $[I_2] = 0$ mol/L (thin line) and $[I_2] = 0.6 \times 10^{-2}$ mol/L (broken line). The parameters of these models are given in the text.

Table I
Some Characteristic Parameters of Amylose Samples at Different Iodine Concentrations

$[I_2]$ concn (mol/L)	R_g (Å)	$I^*(0)^a$	D_{max} (Å)	peak position of $p(r)$ (Å)
AMA, 0.29 (unit mol)/L				
0	20.5 ± 0.6	1	85	20
0.2 × 10^{-2}	38.8 ± 0.8	9.4	157	37
0.6 × 10^{-2}	41.1 ± 0.9	8.9	158	44
AMB, 0.023 (unit mol)/L				
0	58.8 ± 1.2	1	181	62
0.6 × 10^{-3}	57.1 ± 1.2	1.1	177	66
0.2 × 10^{-2}	55.1 ± 1.2	1.1	173	69

[a] The zero-angle scattering intensity $I^*(0)$ is normalized by $I(0)$ at $[I_2] = 0$.

References and Notes

(1) Banks, W., Greenwood, C. T., Eds. *Starch and its Components*; The University Press; Edinburgh, 1975.
(2) (a) Rundle, R. E.; Baldwin, R. R. *J. Am. Chem. Soc.* **1943**, *65*, 554. (b) Rundle, R. E.; Edwards, F. C. *J. Am. Chem. Soc.* **1943**, *65*, 2200. (c) Rundle, R. E.; French, D. *J. Am. Chem. Soc.* **1943**, *65*, 558. (d) Rundle, R. E.; French, D. *J. Am. Chem. Soc.* **1943**, *65*, 1707. (e) Rundle, R. E.; Daasch, L.; French, D. *J. Am. Chem. Soc.* **1944**, *66*, 130. (f) Rundle, R. E.; Foster, J. F.; Baldwin, R. R. *J. Am. Chem. Soc.* **1944**, *66*, 2116. (g) Rundle, R. E. *J. Am. Chem. Soc.* **1947**, *69*, 1769.
(3) Bluhm, T. L.; Zugenmaier, P. *Carbohydr. Res.* **1981**, *89*, 1.
(4) McMullan, R. K.; Saenger, W.; Fayos, J.; Mootz, D. *Carbohydr. Res.* **1973**, *31*, 211.
(5) Noltemeyer, M.; Saenger, W. *Nature* **1976**, *259*, 629.

(6) Noltemeyer, M.; Saenger, W. *J. Am. Chem. Soc.* **1980**, *102*, 2710.
(7) Sano, T.; Yamamoto, M.; Hori, H.; Yasunaga, T. *Bull. Chem. Soc. Jpn.* **1984**, *57*, 678.
(8) Cesàro, A.; Jerian, E.; Saule, S. *Biopolymers* **1980**, *19*, 1491.
(9) Szejtli, J.; Richter, M.; Augustat, S. *Biopolymers* **1967**, *5*, 5.
(10) Amari, T.; Nakamura, M. *J. Appl. Polym. Sci.* **1976**, *20*, 2031.
(11) Teitelbaum, R. C.; Ruby, S. L.; Marks, T. J. *J. Am. Chem. Soc.* **1978**, *100*, 3215.
(12) Heyde, M. E.; Rimai, L.; Kilponen, R. G.; Gill, D. *J. Am. Chem. Soc.* **1972**, *94*, 5222.
(13) Yamamoto, M.; Sano, T.; Harada, S.; Yasunaga, T. *Bull. Chem. Soc. Jpn.* **1983**, *56*, 2643.
(14) Kuge, T.; Ono, S. *Bull. Chem. Soc. Jpn.* **1961**, *34*, 1264.
(15) Manley, R. S. J. *J. Polym. Sci.: Part A* **1964**, *2*, 4503.
(16) Yajima, H.; Nishimura, T.; Ishii, T.; Handa, T. *Carbohydr. Res.* **1987**, *163*, 155.
(17) Pfannemüller, B.; Mayerhöfer, H.; Schulz, R. C. *Biopolymers* **1971**, *10*, 243.
(18) Pfannemüller, B. *Carbohydr. Res.* **1978**, *61*, 41.
(19) Pal, M. K.; Pal, P. K. *Makromol. Chem.* **1987**, *188*, 1735.
(20) Bittiger, H.; Husemann, E.; Pfannemüller, B.; Freiburg, i. Br. *Stärke* **1971**, *23*, 113.
(21) Bittiger, H.; Husemann, E.; Kuppel, A. *J. Polym. Sci., Part C* **1969**, *28*, 45.
(22) Szejtli, J.; Augustat, S.; Richter, M. *Biopolymers* **1967**, *5*, 17.
(23) Dintzis, F. R.; Tobin, R.; Beckwith, A. C. *Macromolecules* **1976**, *9*, 478.
(24) Dintzis, F. R.; Beckwith, A. C.; Babcock, G. E.; Tobin, R. *Macromolecules* **1976**, *9*, 471.
(25) Robin, M. B. *J. Chem. Phys.* **1964**, *40*, 3369.
(26) Handa, T.; Yajima, H. *Biopolymers* **1980**, *19*, 723.
(27) Handa, T.; Yajima, H.; Kajiura, T. *Biopolymers* **1980**, *19*, 1723.
(28) Handa, T.; Yajima, H. *Biopolymers* **1979**, *18*, 873.
(29) Handa, T.; Yajima, H. *Biopolymers* **1981** *20*, 2051.
(30) (a) Minick, M.; Fotta, K.; Khan, A. *Biopolymers* **1991**, *31*, 57. (b) Teitlebaum, R. C.; Ruby, S. L.; Marks, T. J. *J. Am. Chem. Soc.* **1980**, *102*, 3322.
(31) Painter, T. J. *J. Chem. Soc., Perkin Trans. 2* **1976**, 215.
(32) Pal, M. K.; Roy, A. *Makromol. Chem., Rapid Commun.* **1985**, *6*, 749.
(33) Banks, W.; Greenwood, C. T. *Stärke* **1971**, *23*, 222.
(34) Senior, M. B.; Hamori, E. *Biopolymers* **1973**, *12*, 65.
(35) Ueki, T.; Hiiragi, Y.; Izumi, Y.; Tagawa, H.; Kataoka, M.; Muroga, Y.; Matsushita, T.; Amemiya, Y. *Photon Factory Activity Report* KEK Progress Report 83-1; KEK; Tsukuba, Japan, 1984; pp. VI-70-VI-71.
(36) Guinier, A. *Ann. Phys.* **1939**, *12*, 161.
(37) Stuhrmann, H. B.; Kirste, R. G. *Z. Phys. Chem.* **1965**, *46*, 247.

Registry No. I_2, 7553-56-2; KI, 7681-11-0; amylose, 9005-82-7.